Allosteric interactions between agonists and antagonists within the adenosine A_{2A} receptor-dopamine D_2 receptor heterotetramer

Jordi Bonaventura[a,b], Gemma Navarro[a], Verònica Casadó-Anguera[a], Karima Azdad[c], William Rea[b], Estefanía Moreno[a], Marc Brugarolas[a], Josefa Mallol[a], Enric I. Canela[a], Carme Lluís[a], Antoni Cortés[a], Nora D. Volkow[d], Serge N. Schiffmann[c], Sergi Ferré[b,1], and Vicent Casadó[a,1]

[a]Department of Biochemistry and Molecular Biology, Faculty of Biology, University of Barcelona, and Centro de Investigación Biomédica en Red Sobre Enfermedades Neurodegenerativas and Institute of Biomedicine of the University of Barcelona, 08028 Barcelona, Spain; [b]Integrative Neurobiology Section, National Institute on Drug Abuse, Intramural Research Program, National Institutes of Health, Baltimore, MD 21224; [c]Laboratory of Neurophysiology, Universite Libre de Bruxelles-Neuroscience Institute, 1070 Brussels, Belgium; and [d]National Institute on Alcohol Abuse and Alcoholism, National Institutes of Health, Bethesda, MD 20892

Edited by Susan G. Amara, National Institute of Mental Health, Bethesda, MD, and approved May 27, 2015 (received for review April 21, 2015)

Adenosine A_{2A} receptor ($A_{2A}R$)-dopamine D_2 receptor (D_2R) heteromers are key modulators of striatal neuronal function. It has been suggested that the psychostimulant effects of caffeine depend on its ability to block an allosteric modulation within the $A_{2A}R$-D_2R heteromer, by which adenosine decreases the affinity and intrinsic efficacy of dopamine at the D_2R. We describe novel unsuspected allosteric mechanisms within the heteromer by which not only $A_{2A}R$ agonists, but also $A_{2A}R$ antagonists, decrease the affinity and intrinsic efficacy of D_2R agonists and the affinity of D_2R antagonists. Strikingly, these allosteric modulations disappear on agonist and antagonist coadministration. This can be explained by a model that considers $A_{2A}R$-D_2R heteromers as heterotetramers, constituted by $A_{2A}R$ and D_2R homodimers, as demonstrated by experiments with bioluminescence resonance energy transfer and bimolecular fluorescence and bioluminescence complementation. As predicted by the model, high concentrations of $A_{2A}R$ antagonists behaved as $A_{2A}R$ agonists and decreased D_2R function in the brain.

adenosine A_{2A} receptor | dopamine D_2 receptor | caffeine | GPCR heteromers

Most evidence indicates that G protein-coupled receptors (GPCRs) form homodimers and heteromers. Homodimers seem to be a predominant species, and oligomeric entities can be viewed as multiples of dimers (1). It has been proposed that GPCR heteromers are constituted mainly by heteromers of homodimers (1, 2). Allosteric mechanisms determine a multiplicity of unique pharmacologic properties of GPCR homodimers and heteromers (1, 3). First, binding of a ligand to one of the receptors in the heteromer can modify the affinity of ligands for the other receptor (1, 3, 4). The most widely reproduced allosteric modulation of ligand-binding properties in a GPCR heteromer is the ability of adenosine A_{2A} receptor ($A_{2A}R$) agonists to decrease the affinity of dopamine D_2 receptor (D_2R) agonists in the $A_{2A}R$-D_2R heteromer (5). $A_{2A}R$-D_2R heteromers have been revealed both in transfected cells (6, 7), striatal neurons in culture (6, 8) and in situ, in mammalian striatum (9, 10), where they play an important role in the modulation of GABAergic striatopallidal neuronal function (9, 11).

In addition to ligand-binding properties, unique properties for each GPCR oligomer emerge in relation to the varying intrinsic efficacy of ligands for different signaling pathways (1–3). Intrinsic efficacy refers to the power of the agonist to induce a functional response, independent of its affinity for the receptor. Thus, allosteric modulation of an agonist can potentially involve changes in affinity and/or intrinsic efficacy (1, 3). This principle can be observed in the $A_{2A}R$-D_2R heteromer, where a decrease in D_2R agonist affinity cannot alone explain the ability of an $A_{2A}R$ agonist to abolish the decreased excitability of GABAergic striatopallidal neurons induced by high concentration of a D_2R agonist (9), which should overcome the decrease in affinity. Furthermore, a differential effect of allosteric modulations of different agonist-mediated signaling responses (i.e., functional selectivity) can occur within GPCR heteromers (1, 2, 8). Again, the $A_{2A}R$-D_2R heteromer provides a valuable example. A recent study has shown that different levels of intracellular Ca^{2+} exert different modulations of $A_{2A}R$-D_2R heteromer signaling (8). This depends on the ability of low and high Ca^{2+} to promote a selective interaction of the heteromer with different Ca^{2+}-binding proteins, which differentially modulate allosteric interactions in the heteromer (8).

It has been hypothesized that the allosteric interactions between $A_{2A}R$ and D_2R agonists within the $A_{2A}R$-D_2R heteromer provide a mechanism responsible not only for the depressant effects of $A_{2A}R$ agonists, but also for the psychostimulant effects of adenosine $A_{2A}R$ antagonists and the nonselective adenosine receptor antagonist caffeine (9, 11, 12), with implications for several neuropsychiatric disorders (13). In fact, the same mechanism has provided the rationale for the use of $A_{2A}R$ antagonists

Significance

G protein-coupled receptors (GPCRs) constitute the largest plasma membrane protein family involved in cell signaling. GPCR homodimers are predominant species, and GPCR heteromers likely are constituted by heteromers of homodimers. The adenosine A_{2A} receptor ($A_{2A}R$)-dopamine D_2 receptor (D_2R) heteromer is a target for the nonselective adenosine receptor antagonist caffeine. This study uncovers allosteric modulations of $A_{2A}R$ antagonists that mimic those of $A_{2A}R$ agonists, challenging the traditional view of antagonists as inactive ligands. These allosteric modulations disappear when agonist and antagonist are coadministered, however. A model is proposed that considers $A_{2A}R$-D_2R heteromers as heterotetramers, constituted by $A_{2A}R$ and D_2R homodimers. The model predicted that high concentrations of $A_{2A}R$ antagonists would behave as $A_{2A}R$ agonists and decrease D_2R function in the brain.

Author contributions: J.B., G.N., C.L., N.D.V., S.N.S., S.F., and V.C. designed research; J.B., G.N., V.C.-A., K.A., W.R., E.M., M.B., A.C., and V.C. performed research; J.B., G.N., V.C.-A., K.A., W.R., E.M., M.B., J.M., E.I.C., C.L., A.C., S.N.S., S.F., and V.C. analyzed data; and J.B., G.N., C.L., S.N.S., S.F., and V.C. wrote the paper.

The authors declare no conflict of interest.

This article is a PNAS Direct Submission.

[1]To whom correspondence may be addressed. Email: sferre@intra.nida.nih.gov or vcasado@ub.edu.

This article contains supporting information online at www.pnas.org/lookup/suppl/doi:10.1073/pnas.1507704112/-/DCSupplemental.

in patients with Parkinson's disease (13, 14). The initial aim of the present study was to study in detail the ability of caffeine to counteract allosteric modulations between $A_{2A}R$ and D_2R agonists (affinity and intrinsic efficacy) within the $A_{2A}R$-D_2R heteromer. Unexpectedly, when performing control radioligand-binding experiments, not only an $A_{2A}R$ agonist, but also caffeine, significantly decreased D_2R agonist binding. However, when coadministered, the $A_{2A}R$ agonist and caffeine co-counteracted their ability to modulate D_2R agonist binding. By exploring the molecular mechanisms behind these apparent inconsistencies, the present study provides new insight into the quaternary structure and function of $A_{2A}R$-D_2R heteromers.

Results

Caffeine Modulates D_2R Agonist Binding: A New Biochemical Property of the $A_{2A}R$-D_2R Heteromer. As expected, the $A_{2A}R$ agonist CGS 21680 significantly decreased D_2R agonist [^{3}H]quinpirole binding in membrane preparations from both sheep striatum (Fig. 1*A*, black bars) and Chinese hamster ovary (CHO) cells transiently transfected with $A_{2A}R$ and D_2R (Fig. 1*A*, red bars). Unexpectedly, caffeine also produced the same effect (Fig. 1*B*), and the effective concentrations of CGS 21680 and caffeine were in the same range as those able to displace the binding of the selective $A_{2A}R$ antagonist [^{3}H]ZM 241385 in the respective preparations (Fig. S1 *A* and *B*). In transfected cells, the average B_{max} value for [^{3}H]ZM 241385 binding was 1.6 pmol/mg of protein, and that for [^{3}H]raclopride binding was 0.7 pmol/mg of protein. In sheep striatum, the respective average values were 1.8 and 0.4 pmol/mg protein. The decrease in [^{3}H]quinpirole binding by CGS 21680 and caffeine was related to a noncompetitive inhibition, with decreasing affinity (i.e., increase in K_{D1} values), as shown in competition experiments of [^{3}H]quinpirole vs. quinpirole (Table 1).

Previous studies have shown that in the $A_{2A}R$-D_2R heteromer, a strong electrostatic interaction occurs between an arginine-rich epitope localized in the N-terminal part of the third intracellular loop of the D_2R and a phosphorylated residue, serine-374, localized in the distal part of the C terminus of the $A_{2A}R$ (15, 16). Bioluminescence energy transfer experiments demonstrated that transfection with mutant $A_{2A}R$ ($A_{2A}^{A374}R$) or D_2R lacking these key interacting residues leads to pronounced modification of the quaternary structure of the heteromer (15, 17, 18). In transfected cells, $A_{2A}^{A374}R$ showed a very similar expression (B_{max} for [^{3}H]ZM 241385 binding of 2.0 pmol/mg protein) and the same affinity for caffeine or CGS 21680 compared with the wild-type $A_{2A}R$. Identical competition curves of [^{3}H]ZM 241385 vs. CGS 21680 or caffeine were obtained from cells transfected with D_2R and either $A_{2A}^{A374}R$ or wild-type $A_{2A}R$ (Fig. S1*B*). The ability of CGS 21680 and caffeine at modulating [^{3}H]quinpirole binding was significantly reduced in the CHO cells transfected with D_2R and the mutant $A_{2A}^{A374}R$, however (Fig. 1 *A* and *B*, blue bars). This indicates that the allosteric modulations between an $A_{2A}R$ agonist or antagonist and a D_2R agonist depend on the quaternary structure of the $A_{2A}R$-D_2R, determined by the electrostatic interaction between intracellular domains of both receptors, and thus constitute a biochemical property of the $A_{2A}R$-D_2R heteromer.

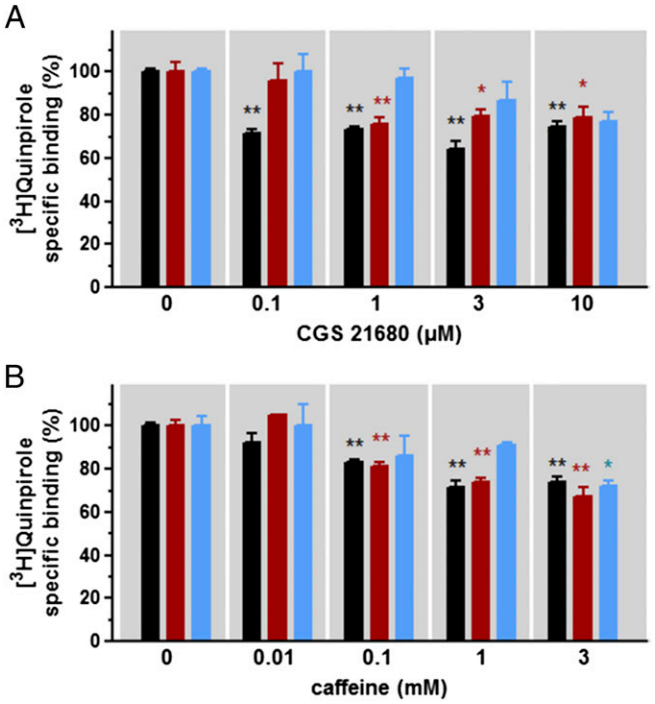

Fig. 1. Effect of an $A_{2A}R$ agonist and caffeine on [^{3}H]quinpirole binding to D_2R. [^{3}H]Quinpirole binding (6 nM) was determined in membrane preparations from sheep striatum (black bars) or CHO cells transfected with D_2R cDNA (2 μg) and $A_{2A}R$ cDNA (3 μg) (red bars) or D_2R cDNA (2 μg) and cDNA (3 μg) from mutated $A_{2A}R$ ($A_{2A}^{A374}R$; blue bars) in the presence or the absence of increasing concentrations of the $A_{2A}R$ agonist CGS21680 (*A*) or caffeine (*B*). Values are mean ± SEM from between three and five different experiments of relative [^{3}H]quinpirole-specific binding (% of nontreated membranes). Statistical significance was calculated by one-way ANOVA followed by Dunnett's post hoc test. *P < 0.05; **P < 0.01, compared with nontreated membrane preparations.

$A_{2A}R$ Agonists and Antagonists Cocounteract Their Ability to Modulate D_2R Agonist Binding and Function: Two $A_{2A}R$ Protomers in the $A_{2A}R$-D_2R Heteromer. Because both $A_{2A}R$ agonists and antagonists produce a conformational change in the $A_{2A}R$-D_2R heteromer that leads to the same effect, a reduced affinity of agonists for D_2R (Table 1), this questions the validity of the allosteric interactions between $A_{2A}R$ and D_2R agonists as a main mechanism involved in the opposite and counteracting behavioral effects of $A_{2A}R$ agonists and antagonists. We evaluated the combined effect of $A_{2A}R$ agonists and caffeine or selective $A_{2A}R$ antagonists on D_2R agonist binding. [^{3}H]Quinpirole binding in membrane preparations from sheep striatum was measured in the presence of CGS 21680 (100 nM) and increasing concentrations of caffeine (Fig. 2*A*) or the selective $A_{2A}R$ antagonists SCH 58261 (Fig. 2*C*) and KW 6002 (Fig. 2*E*). Caffeine and the selective $A_{2A}R$ antagonists produced a biphasic effect on the ability of CGS 21680 to decrease [^{3}H]quinpirole binding. Low concentrations counteracted the effect of CGS 21680, whereas high concentrations were associated with a significant decrease in [^{3}H]quinpirole binding. These results show that $A_{2A}R$ agonists and antagonists that bind competitively to the orthosteric site (19–21) produce the same allosteric modulation of D_2R agonist binding when individually administered, and yet they can cancel each other's effect when coadministered. This strongly suggests the presence of the

Table 1. Effect of $A_{2A}R$ ligands on [^{3}H]quinpirole and [^{3}H]raclopride affinity for D_2R

Treatment	[^{3}H]Quinpirole-binding K_{DA1}, nM	[^{3}H]Raclopride-binding K_{DA1}, nM
Control	5 ± 2	1.8 ± 0.7
CGS 21680 (3 μM)	10 ± 2*	4.2 ± 0.7*
Caffeine (3 mM)	14 ± 3*	3.7 ± 0.7*

K_{DA1} is the equilibrium dissociation constant. Values are mean ± SEM from three to five different experiments. Statistical significance was calculated using the Student *t* test. *P < 0.05 compared with controls.

$A_{2A}R$ homodimer with two orthosteric binding sites. A corollary of this assumption would be that simultaneous occupancy of the $A_{2A}R$ homodimer in the $A_{2A}R$-D_2R heteromer by an agonist and an antagonist should not induce an allosteric modulation of D_2R agonist binding.

The dimeric nature of the $A_{2A}R$ was confirmed with dissociation experiments of [^{3}H]ZM 241385 in sheep striatal preparations. The $A_{2A}R$ agonist CGS 21680, but not caffeine or SCH 58261, significantly modified the dissociation rate of the labeled antagonist (Fig. 3), indicating formation of a hybrid species with both agonist and antagonist simultaneously binding to the dimer. Therefore, only the agonist can exert an allosteric modulation of the labeled antagonist when both are occupying orthosteric sites in an $A_{2A}R$ oligomer, because the four ligands—caffeine, ZM 241385, SCH 58261, and CGS 21680—all bind and compete for the same orthosteric site (19–21). This implies a different conformation of the $A_{2A}R$ homodimer when occupied simultaneously with an agonist and an antagonist compared with when occupied with two antagonists. This different conformation could then explain the differential ability of the $A_{2A}R$ homodimer, when occupied only by an agonist or an antagonist or simultaneously by an agonist and antagonist, to allosterically modulate D_2R agonist binding and intrinsic efficacy within the $A_{2A}R$-D_2R heteromer.

The same allosteric modulation exerted by $A_{2A}R$ agonists and antagonists on D_2R agonist affinity was also evident on

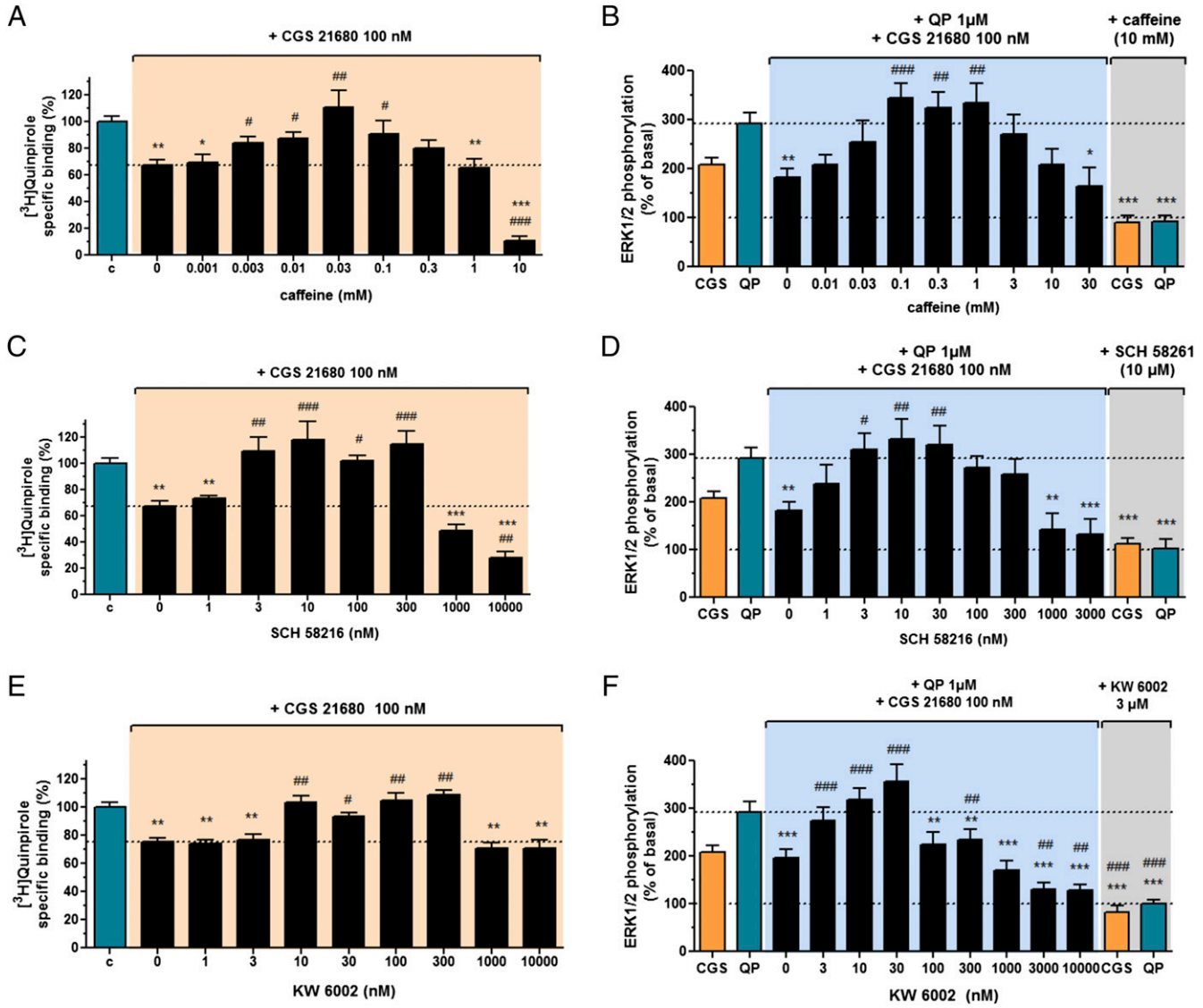

Fig. 2. Biphasic effect of caffeine and selective $A_{2A}R$ antagonists on [^{3}H]quinpirole binding and D_2R-mediated ERK1/2 phosphorylation. (*A*, *C*, and *E*) [^{3}H]Quinpirole binding (6 nM) was determined in membrane preparations from sheep striatum not preincubated (control, blue bars) or preincubated (black bars) for 30 min with the $A_{2A}R$ agonist CGS 21680 (100 nM) and increasing concentrations of caffeine (*A*) or the selective $A_{2A}R$ antagonists SCH 58216 (*C*) or KW 6002 (*E*). Values are mean ± SEM from four to eight different experiments of relative [^{3}H]quinpirole binding (% of nontreated control membranes, c). Statistical significance was calculated by one-way ANOVA followed by the Newman–Keuls post hoc test. $^*P < 0.05$; $^{**}P < 0.01$; $^{***}P < 0.001$, compared with c. $^{\#}P < 0.05$; $^{\#\#}P < 0.01$; $^{\#\#\#}P < 0.001$ compared with only CGS 21680. (*B*, *D*, and *F*) ERK1/2 phosphorylation was determined in HEK-293 cells transfected with D_2R cDNA (0.8 μg) and $A_{2A}R$ cDNA (1.2 μg), stimulated for 5 min with CGS 21680 (CGS; 100 nM) or quinpirole (QP; 1 μM) alone (orange and blue bars, respectively) or in combination (black bars) after incubation for 10 min with vehicle or with caffeine (*B*), SCH 58126 (*D*), or KW 6002 (*F*). ERK1/2 phosphorylation was quantified; values represent mean ± SEM from three to six different experiments of the percentage of phosphorylation relative to basal levels in nontreated cells (100%). Statistical significance was calculated by one-way ANOVA followed by Dunnett's post hoc test. $^*P < 0.05$; $^{**}P < 0.01$; $^{***}P < 0.001$, compared with QP. $^{\#}P < 0.05$; $^{\#\#}P < 0.01$; $^{\#\#\#}P < 0.001$, compared with cells treated with QP plus CGS.

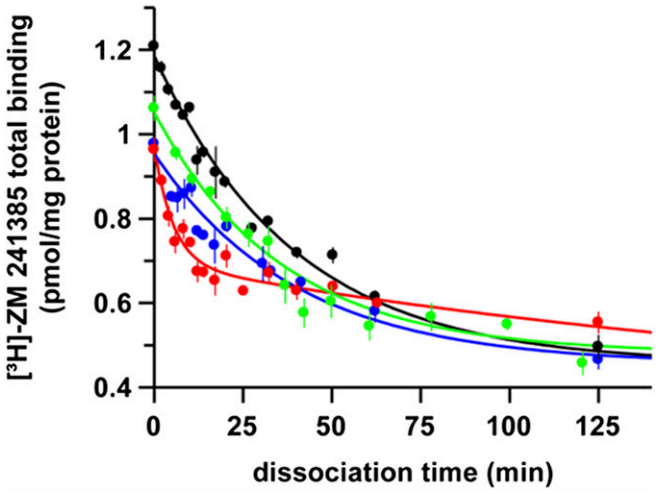

Fig. 3. Dissociation kinetics of [^{3}H]ZM 241385 in the presence of caffeine or selective $A_{2A}R$ ligands. Dissociation curves of the $A_{2A}R$ antagonist [^{3}H]ZM 241385 (1.5 nM) in the absence (black curve) or presence of either the $A_{2A}R$ antagonists SCH 58260 (10 nM, blue curve) or caffeine (30 μM, green curve), or the $A_{2A}R$ agonist CGS 21680 (10 nM, red curve). Data points are means ± SD of triplicates. Fitted K_{off} values of [^{3}H]ZM 241385 dissociation were 0.025 ± 0.002 min^{-1} (i.e., a residence time of 40 min) for control, 0.025 ± 0.003 min^{-1} (residence time of 40 min) in the presence of SCH 58260, and 0.028 ± 0.004 min^{-1} (residence time of 36 min) in the presence of caffeine. A biphasic curve was obtained in the presence of CGS 21680 (red curve) with a K_{off1} value of 0.19 ± 0.03 min^{-1} and a K_{off2} value of 0.004 ± 0.003 min^{-1} (residence time of 5 and 250 min, respectively).

D_2R agonist intrinsic efficacy. In HEK-293 cells transfected with $A_{2A}R$ and D_2R, quinpirole (1 μM) and CGS 21680 (100 nM) produced increases in ERK1/2 phosphorylation over basal levels of approximately 300% and 200%, respectively (Fig. 2*B*). The effect of quinpirole was partially but significantly counteracted by CGS 21680 to the levels of ERK1/2 phosphorylation induced by CGS 21680 alone. Given that the high concentration of quinpirole used (1 μM) should overcome the decrease in affinity induced by CGS 21680 (100 nM) (Table 1), this indicates the ability of the $A_{2A}R$ agonist to decrease not only D_2R agonist affinity, but also its intrinsic efficacy, as previously shown in electrophysiological experiments on striatal neurons (9). Increasing concentrations of caffeine (Fig. 2*B*), SCH 58261 (Fig. 2*D*), or KW 6002 (Fig. 2*F*) produced the same biphasic effect as seen in the radioligand-binding experiments (Fig. 2): low concentrations counteracted the effect of CGS 21680, and this effect disappeared with larger concentrations, when caffeine, SCH 58261, and KW 6002 by themselves completely antagonized the effect of both CGS 21680 and quinpirole. Therefore, simultaneous occupancy of the $A_{2A}R$ homodimer in the $A_{2A}R$-D_2R heteromer by an agonist and an antagonist blocks the allosteric modulation of both D_2R agonist binding and intrinsic efficacy. Considering that there is a tone of adenosine under physiological conditions, this in fact could be the main mechanism by which caffeine and $A_{2A}R$ antagonists counteract the functional and behavioral effects that depend on D_2R signaling by the $A_{2A}R$-D_2R heteromer.

$A_{2A}R$-D_2R Heteromers Assemble Into Tetrameric Complexes. A bimolecular luminescence and fluorescence complementation approach was used to demonstrate the ability of $A_{2A}R$ and D_2R to form heterotetramers. First, in HEK-293 cells, *Renilla* luciferase (Rluc) reconstitution after transfection of $A_{2A}R$ fused to the Rluc N-terminal hemiprotein ($A_{2A}R$-nRluc) and D_2R fused to the Rluc C-terminal hemiprotein (D_2R-cRluc) was demonstrated by strong bioluminescence after addition of the Rluc substrate coelenterazine H, indicating $A_{2A}R$(nRluc)-D_2R(cRluc) heteromerization (Fig. S2). A_1R-D_2R and $A_{2A}R$-D_1R pairs (fused to corresponding hemiproteins) served as negative controls, in agreement with the suggested ability of $A_{2A}R$ to heteromerize with D_2R and not with D_1R and with the ability of D_2R to heteromerize with $A_{2A}R$ and not with A_1R (6, 22) (Fig. S2).

Second, significant fluorescence could be observed when HEK-293 cells were transfected with $A_{2A}R$ fused to the YFP Venus N-terminal hemiprotein ($A_{2A}R$-nYFP) and with D_2R fused to the YFP Venus C-terminal hemiprotein (D_2R-cYFP), indicating YFP reconstitution and therefore $A_{2A}R$(nYFP)-D_2R(cYFP) heteromerization (Fig. 4*A*). A_1R-D_2R and $A_{2A}R$-D_1R pairs (fused to corresponding hemiproteins) served as negative controls here as well (Fig. 4*A*).

Finally, complemented Rluc from $A_{2A}R$(nRluc)-D_2R(cRluc) heteromers and complemented YFP from $A_{2A}R$(nYFP)-D_2R (cYFP) heteromers were used as donor and acceptor molecules in bioluminescence resonance energy transfer (BRET) experiments (Fig. 4*B*). Significant BRET values were obtained with cotransfection of $A_{2A}R$-nRluc, D_2R-cRluc, $A_{2A}R$-nYFP, and D_2R-cYFP (Fig. 4*B*). A_1R-D_2R and $A_{2A}R$-D_1R pairs (fused to corresponding hemiproteins) again served as negative controls (Fig. 4*B*). Further controls included independent experiments replacing each receptor fused to its hemiprotein with the same nonfused (soluble) hemiprotein (Table S1).

Bimolecular fluorescence complementation was also used to evaluate the ability of peptides with the amino acid sequence of transmembrane domains (TMs) to destabilize $A_{2A}R$-D_2R heteromers, as recently described for dopamine D_1R-D_3R heteromers (2). Previous BRET experiments with disrupting peptides had suggested the involvement of TM5 from D_2R in $A_{2A}R$-D_2R heteromerization (18). We investigated whether synthetic peptides with the sequence of TM5 and TM7 of $A_{2A}R$ or D_2R fused to HIV TAT were able to destabilize receptor heteromerization. Both TM5 peptides, but none of the TM7 peptides, reduced fluorescence complementation in cells expressing $A_{2A}R$-nYFP and D_2R-cYFP (Fig. 4*A*), suggesting that, in addition to intracellular domains, TM5 forms part of the heteromerization interface. In contrast, neither TM5 or TM7 from $A_{2A}R$ or D_2R was able to decrease fluorescence complementation in cells expressing $A_{2A}R$-nYFP and $A_{2A}R$-cYFP or D_2R-nYFP and D_2R-cYFP (Fig. 4*A*), supporting the selective involvement of TM5 on the heteromer interface.

Pharmacologic Evidence for $A_{2A}R$ Agonist/Antagonist-Mediated Allosteric Modulation of D_2R Function in Striatal Cells and in the Experimental Animal. Previous patch-clamp experiments in rat striatal slices showed that CGS 21680 completely antagonizes the decrease of neuronal excitability (i.e., NMDA-induced neuronal firing) induced by D_2R agonists, which was demonstrated to depend on an allosteric modulation of D_2R agonist efficacy and on $A_{2A}R$-D_2R heteromerization (9). It was also shown that SCH 58261 counteracts the allosteric effect of CGS 21680 on D_2R function (9), but the effect of the $A_{2A}R$ antagonist alone was not analyzed. Under these experimental conditions, the slice bathing solution is free of endogenous neurotransmitters, thereby allowing testing in situ of the $A_{2A}R$ agonist/antagonist-mediated allosteric modulation of D_2R function without the interference of endogenous adenosine. We first reproduced the effect of NMDA (5 μM; increase in neuronal firing) and the counteraction of this effect by the D_2R agonist agonist R(−)-propylnorapomorphine hydrochloride (NPA; 10 μM) (Fig. 5*A*). Remarkably, the $A_{2A}R$ antagonist SCH 58261 (1 μM) completely counteracted the effect of the D_2R agonist (Fig. 5 *A* and *B*), as reported for CGS 21680. These results mirror those obtained with transfected cells and demonstrate that both $A_{2A}R$ agonists and antagonists are able to modulate D_2R function in the striatum.

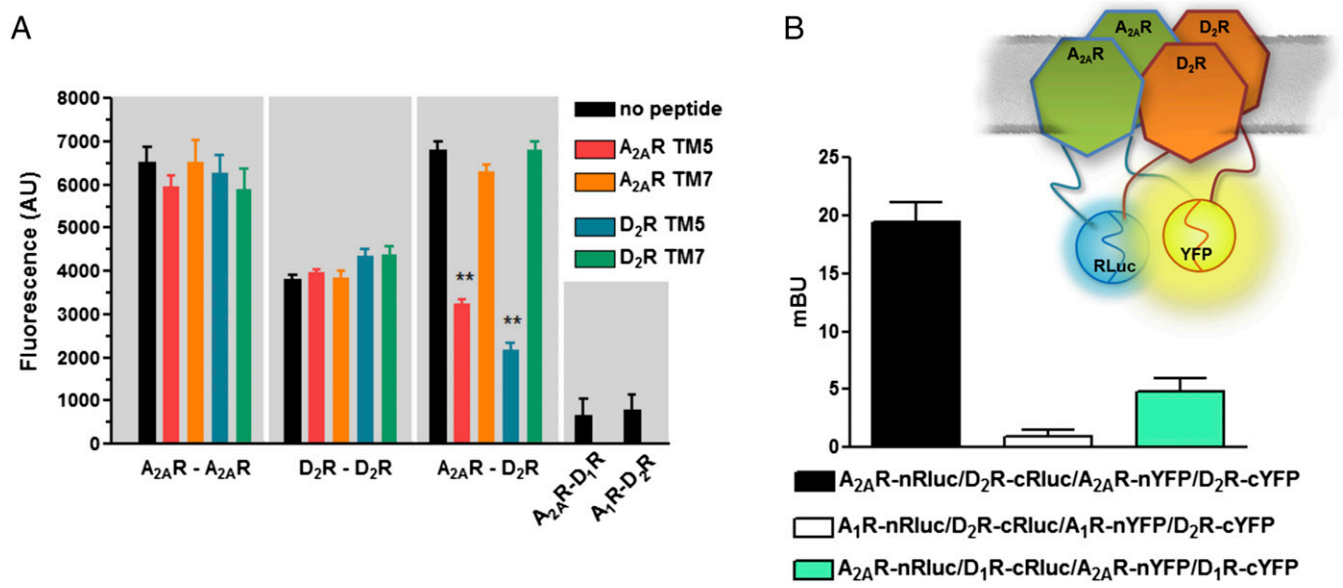

Fig. 4. Tetrameric structure of the $A_{2A}R$-D_2R heteromer. (*A*) Fluorescence due to complementation [in arbitrary units (AU)] of YFP Venus was determined in HEK-293 cells coexpressing $A_{2A}R$-nYFP and $A_{2A}R$-cYFP, D_2R-nYFP and D_2R-cYFP, or $A_{2A}R$-nYFP and D_2R-cYFP either not treated or treated with the indicated HIV TAT peptides (4 μM) for 4 h. Values represent means ± SEM from seven or eight different experiments. Statistical significance was calculated by one-way ANOVA followed by Dunnett's post hoc test. $^{**}P < 0.01$, compared with the nontreated cells. (*B*) BRET was determined in cells expressing $A_{2A}R$-nRluc, D_2R-cRluc, $A_{2A}R$-nYFP and D_2R-cYFP, or $A_{2A}R$-nYFP and D_2R-cYFP and the respective controls replacing $A_{2A}R$ for A_1R or D_2R for D_1R. Values are mean ± SEM of three different experiments. (*Upper*) Schematic representation of BRET with bimolecular luminescence and fluorescence complementation.

It is well known that locomotor activation by $A_{2A}R$ antagonists or caffeine shows an inverted U-shaped dose–response curve, with a depressant effect at high doses (23–25). This depressant effect could be related to the ability of the antagonists to largely displace endogenous adenosine and occupy both protomers in the $A_{2A}R$ homodimer of the $A_{2A}R$-D_2R hetero-

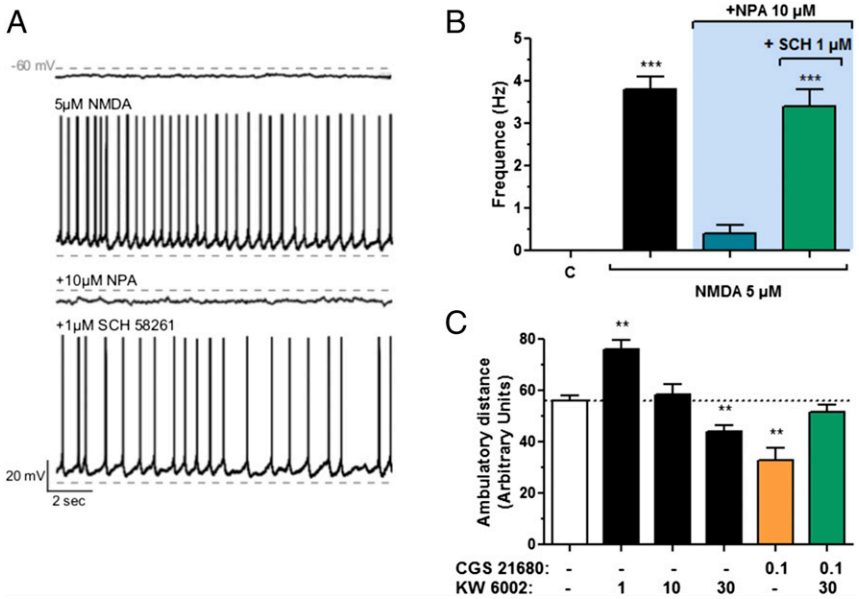

Fig. 5. Allosteric modulation of $A_{2A}R$ antagonists on D_2R-mediated modulation of neuronal function. (*A* and *B*) Effect of the A_2R antagonist SCH 58261 on NMDA-mediated depolarized plateau potential on D_2R-responsive neurons in rat ventral striatal slices. (*A*) Consecutive traces showing typical transitions where the action of NMDA (5 μM) was recorded before and in the presence of D_2R NPA (10 μM) and the $A_{2A}R$ antagonist SCH 58261 (1 μM). On a D_2R-responsive neuron, subsequent application of SCH 58261 totally counteracts the effect of NPA, i.e., inhibition of the depolarized plateau potential and firing frequency. (*B*) Summary histogram obtained from D_2R-responsive neurons illustrating the antagonistic effect of SCH 58261 on the action potential firing frequency. Data represent mean ± SEM ($n = 7$). Statistical significance was calculated by one-way ANOVA followed by Dunnett's post hoc test. $^{***}P < 0.001$, compared with the untreated slice preparation (c). (*C*) Locomotor activity in nonhabituated rats during the first 20 min after the administration of vehicle or the $A_{2A}R$ antagonist KW 6002 (1–30 mg/kg, i.p.). The $A_{2A}R$ agonist CGS 21680 (0.1 mg/kg i.p.), or vehicle, was administered 30 min before the administration of KW 6002. A high dose of KW 6002 produced significant locomotor depression, which was counteracted by a previous administration of the additional depressant dose of CGS 21680. Statistical significance was calculated by one-way ANOVA followed by Dunnett's post hoc test. $^{**}P < 0.01$ compared with controls (animals only treated with vehicle).

mer. In that case, we would predict that coadministration of a depressant dose of an $A_{2A}R$ agonist should not produce more depression, but rather should counteract the depressant effect of the antagonists. We tested locomotor activity in rats during the first 20 min of activity of nonhabituated animals with doses of the $A_{2A}R$ antagonist KW 6002 above 1 mg/kg, reportedly the maximal effective dose (23). KW 6002 also produced a biphasic effect on D_2R binding and MAPK signaling (Fig. 2*F*), and it was selected because of its pronounced locomotor effects compared with SCH 58261 (23). At 10 mg/kg, KW 6002 did not produce any activation, and at 30 mg/kg it had a depressant effect (Fig. 5*C*). As predicted, coadministration of a depressant dose of CGS 21680 (0.1 mg/kg) (24) counteracted the depressant effect of KW 6002 (30 mg/kg) (Fig. 5*C*). The same dose of CGS 21680 did not significantly counteract (although it did not potentiate) the motor depressant effects of high doses of caffeine (56 and 100 mg/kg) (Fig. S3). Thus, these results agree with previous studies indicating that mechanisms other than adenosine receptor antagonism are involved in the depressant effects of high doses of caffeine (25).

$A_{2A}R$ Agonists and Antagonists Also Modulate D_2R Antagonist Binding in the $A_{2A}R$-D_2R Heteromer. Because both $A_{2A}R$ agonists and antagonists can allosterically modulate the affinity and intrinsic efficacy of D_2R agonists, we questioned whether $A_{2A}R$ ligands also could modulate the binding of D_2R antagonists in the $A_{2A}R$-D_2R heteromer. We found that both CGS 21680 and caffeine significantly reduced [^{3}H]raclopride binding in membrane preparations from sheep and human striatum and from CHO cells transfected with $A_{2A}R$ and D_2R (Fig. 6 *A* and *B*). The decrease in [^{3}H]raclopride binding by CGS 21680 and caffeine was related to a decrease in the affinity of D_2R antagonist (increase in K_{D1} values), as shown in competition experiments (sheep striatum) of [^{3}H]raclopride vs. raclopride (Table 1). As

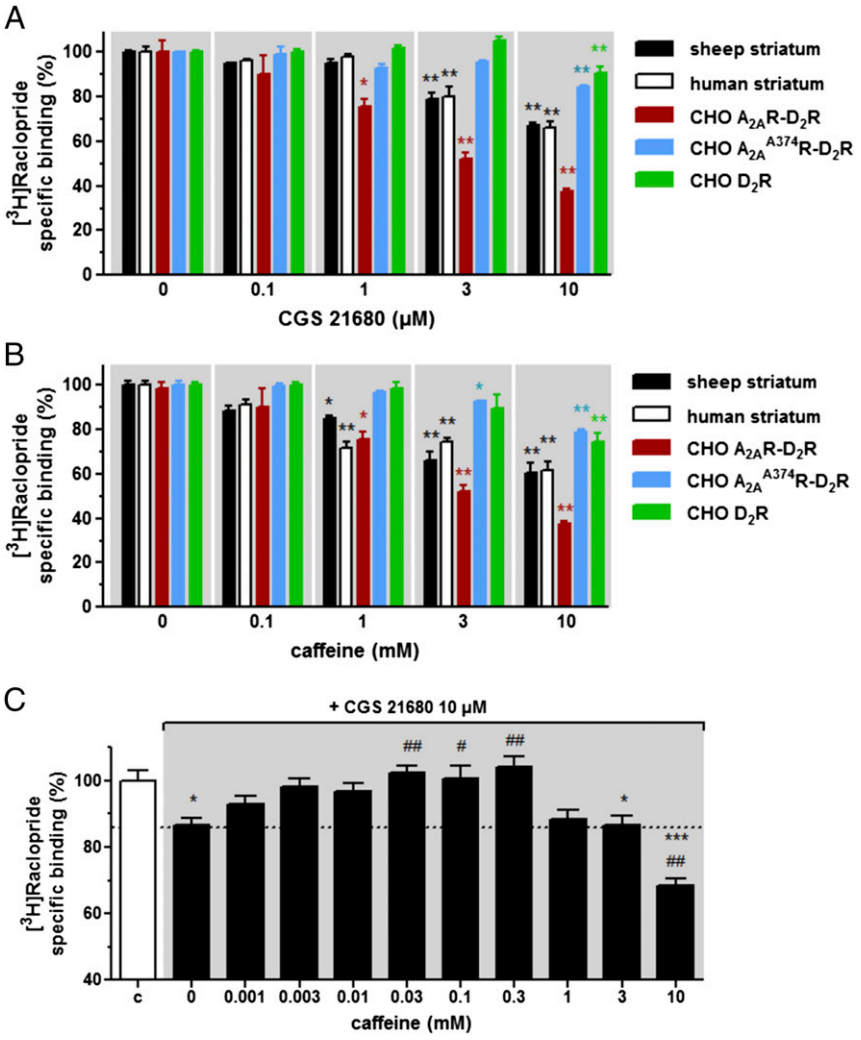

Fig. 6. Effect of an $A_{2A}R$ agonist and caffeine on [^{3}H]raclopride binding. (*A* and *B*) [^{3}H]Raclopride (4 nM) binding was determined in membrane preparations from sheep striatum (black bars), human caudate nucleus (white bars), or CHO cells transfected with D_2R cDNA (2 μg) and $A_{2A}R$ cDNA (3 μg; red bars), D_2R cDNA (2 μg) and cDNA (3 μg) from mutated $A_{2A}R$ ($A_{2A}{}^{A374}R$; blue bars), or CHO cells transfected only with D_2R cDNA (2 μg; green bars) in the presence or the absence of increasing concentrations of the $A_{2A}R$ agonist CGS21680 (*A*) or caffeine (*B*). (*C*) [^{3}H]raclopride (4 nM) binding determined in membrane preparations from sheep striatum either untreated (white bar, c) or treated with CGS 21680 (10 μM) in the absence or presence of increasing concentrations of caffeine (black bars). Values are mean ± SEM from three to five different experiments) of the relative [^{3}H]raclopride-specific binding (% of nontreated membranes). Statistical significance was calculated by one-way ANOVA followed by Dunnett's post hoc test or the Newman–Keuls post hoc test. $^*P < 0.05$; $^{**}P < 0.01$; $^{***}P < 0.001$, compared with the untreated membrane preparations. $^{\#}P < 0.05$; $^{\#\#}P < 0.01$, compared with the membranes treated only with CGS 21680.

controls of adenosine receptor selectivity, neither the A_1R agonist CCPA nor the A_1R antagonist DPCPX modulated [^{3}H]raclopride binding at concentrations that do not bind to $A_{2A}R$ (Fig. S4). Again, the potency of both CGS 21680 and caffeine in modulating [^{3}H]raclopride binding was significantly reduced in cells expressing the mutant $A_{2A}{}^{A374}R$, indicating dependence on $A_{2A}R$-D_2R heteromerization (Fig. 6 *A* and *B*). In fact, the same reduction in the potency of CGS 21680 and caffeine observed in cells expressing the mutant $A_{2A}{}^{A374}R$ was observed in cells transfected only with D_2R (Fig. 6 *A* and *B*), which were found to constitutively express relatively low levels of $A_{2A}R$ (B_{max} for [^{3}H]ZM 241385 binding of 0.25 pmol/mg protein). Furthermore, the same biphasic effect observed with increasing concentrations of caffeine on the ability of the $A_{2A}R$ agonist CGS 21680 to decrease [^{3}H]quinpirole binding was also observed with [^{3}H]raclopride binding in membrane preparations from sheep striatum (Fig. 6*C*) Thus, low concentrations of caffeine antagonized the effect of CGS 21680, whereas high concentrations were also associated with a significant decrease in [^{3}H]raclopride binding (Fig. 6*C*).

We then used disrupting TM peptides to demonstrate that heteromerization is involved in the $A_{2A}R$ ligand-mediated modulation of D_2R binding in striatal tissue. We first checked endogenous $A_{2A}R$-D_2R heteromer expression in sheep striatal slices by a proximity ligation assay (PLA). This technique permits the detection of molecular interactions between two endogenous proteins and it is similar to immunoprecipitation, but with the additional advantage of not requiring membrane

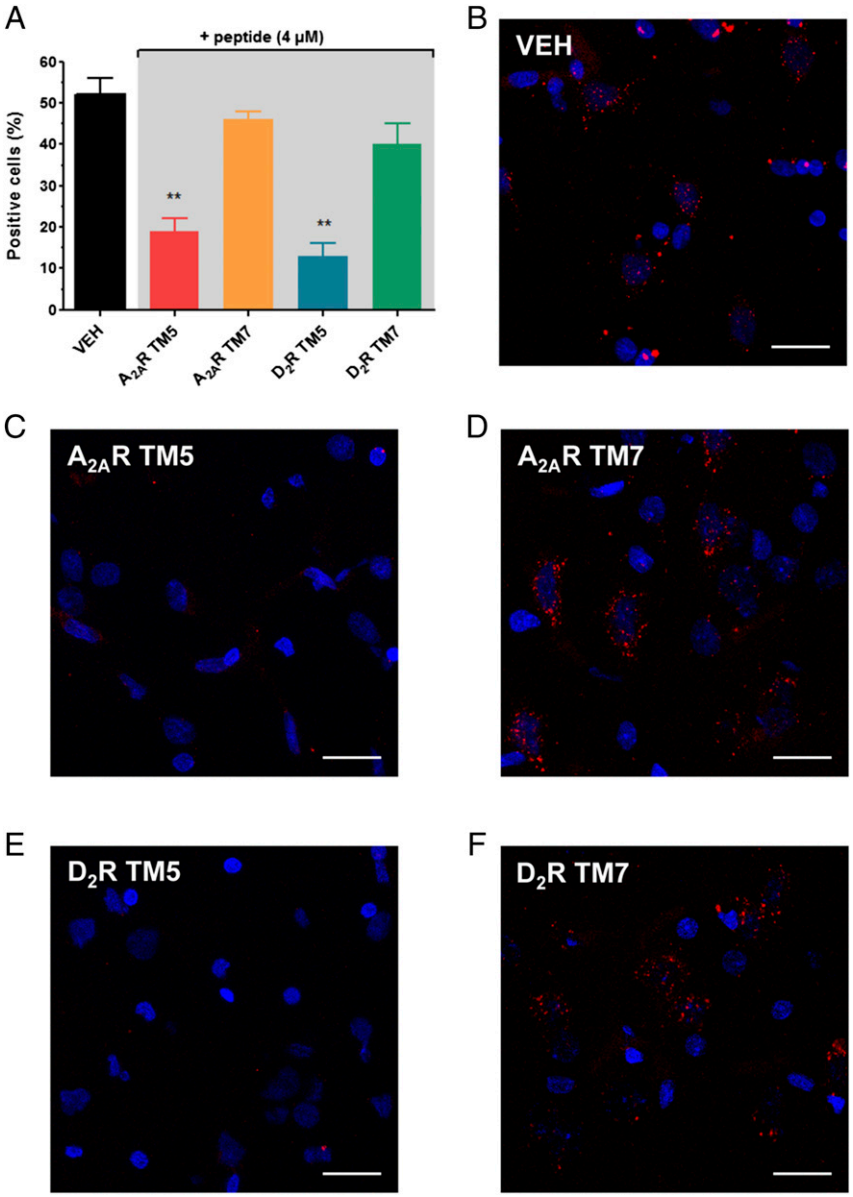

Fig. 7. Detection of $A_{2A}R$-D_2R heteromers in sheep striatum and effect of HIV TAT-TM peptides. The PLA was performed in coronal slices from sheep striatum treated with vehicle or with HIV TAT-fused TM peptides (4 μM) corresponding to TM5 or TM7 of $A_{2A}R$ or D_2R. (*A*) Number of cells containing one or more red spots expressed as the percentage of the total number of cells (blue nucleus). Data (% of positive cells) are the mean ± SEM of counts from a total of 800–1,000 cells, considering between five and 12 different fields. Statistical significance was calculated by one-way ANOVA followed by Dunnett's post hoc test. $^{**}P < 0.01$, compared with the slices treated with vehicle (c). (*B–F*) Representative confocal microscopy images from each experimental condition, in which heteromers appear as red spots. In all cases, cell nuclei were stained with DAPI (blue). (Scale bars: 20 μm.)

solubilization. Labeling heterodimers by PLA requires that both receptors be sufficiently close to allow the two antibody-DNA probes to form double-stranded segments (<16 nm) (10), a signal that is further amplified in the presence of fluorescent nucleotides (Fig. 7). On the PLA, $A_{2A}R$-D_2R heteromers were observed as red punctate staining in slices treated with vehicle or with TM7 peptides, but not in slices treated with TM5 peptides from $A_{2A}R$ or D_2R (Fig. 7 *C* and *E*). Because TM5 peptides disrupted both fluorescence complementation (Fig. 3*A*) and the PLA signal (Fig. 7), we expected that this alteration of the quaternary structure should result in the loss of the allosteric interactions within the heteromer. Indeed, TM5 peptides from both $A_{2A}R$ (Fig. 8*A*) and D_2R (Fig. 8*B*), but not TM7 peptides, counteracted caffeine-mediated decrease in [^{3}H]raclopride binding in sheep striatal membrane preparations (Fig. 8).

Discussion

Several conclusions can be drawn from this study. First, any orthosteric $A_{2A}R$ ligand, agonist or antagonist, can decrease the affinity and intrinsic efficacy of any D_2R ligand. These features constitute biochemical properties of the $A_{2A}R$-D_2R heteromer, because they depend on the integrity of the right quaternary structure of the heteromer, as demonstrated in transfected mammalian cells and striatal tissue, by using heteromer-disrupting mutations and peptides, respectively. Second, the results from radioligand dissociation and double complementation of BRET donor and acceptor units provide strong evidence for a tetrameric structure of the $A_{2A}R$-D_2R heteromer constituted by $A_{2A}R$ and D_2R homodimers. Third, the $A_{2A}R$-D_2R heterotetramer offers a model that explains the apparent contradiction of orthosteric $A_{2A}R$ agonists and antagonists being able to produce the same modulatory effects on D_2R function and yet counteract each other's effects. The model assumes that occupancy of the $A_{2A}R$ homodimer with either an agonist or an antagonist produces a conformational change that conduces the same allosteric modulation to the D_2R, whereas simultaneous occupancy of the $A_{2A}R$ homodimer by an agonist and an antagonist would not allow this conformational change (as indicated by dissociation experiments with the radiolabeled $A_{2A}R$ antagonist).

The model has important heuristic value. As the model predicted, in the brain, under specific pharmacologic conditions, orthosteric $A_{2A}R$ antagonists behave as $A_{2A}R$ agonists and decrease D_2R function, effects that can be counteracted by coadministration of both $A_{2A}R$ agonists and antagonists (electrophysiological and locomotor activity experiments). Given the tone of adenosine under physiological conditions, this in fact could be the main mechanism by which caffeine and $A_{2A}R$ antagonists produce locomotor activation, by counteracting the functional effects that depend on D_2R signaling by the $A_{2A}R$-D_2R heteromer. Nevertheless, motor depression by caffeine or $A_{2A}R$ antagonists implies a significant displacement of endogenous adenosine and occupancy of the $A_{2A}R$ homodimer in the $A_{2A}R$-D_2R heteromer, which can be attained only by high concentrations of caffeine that cannot be obtained through habitual consumption of coffee. Thus, a 12-oz cup of coffee may contain between 107 and 420 mg of caffeine (26), and oral doses of 250 and 500 mg (human adults) produce peak plasma levels of approximately 0.03 and 0.06 mM (27), which is in the range of concentrations at which caffeine counteracts the allosteric effects of CGS 21680 in the present radioligand-binding experiments (Figs. 2*A* and 6*C*). However, therapeutic doses of more potent and selective $A_{2A}R$ antagonists may have differential effects depending on their $A_{2A}R$ affinity and on the levels of endogenous adenosine. Therefore, our model still provides support for the use of $A_{2A}R$ antagonists in treating patients with Parkinson's disease. In addition, the complementing results obtained from functional experiments in mammalian cells in culture, in striatal slices, and in the intact experimental animal provide a basis for understanding the previously claimed significant dependence of D_2R signaling and $A_{2A}R$-D_2R heteromerization on the pharmacologic effects of caffeine and other $A_{2A}R$ ligands (9, 11–13).

Finally, the present results indicate that a large proportion of D_2R forms heteromers with $A_{2A}R$ in transfected cells and striatal tissue. A similar degree of allosteric modulation of D_2R by $A_{2A}R$ ligands was observed in both artificial and native systems. Particularly notorious was the ability of caffeine to allosterically (noncompetitively) decrease D_2R antagonist binding by approximately 60% and 40% in membrane preparations of transfected cells and striatal tissue, respectively. Furthermore, the experiments with MAPK signaling in transfected cells and the electrophysiological experiments in striatal neurons demonstrate an additional strong allosteric modulation of $A_{2A}R$ ligands on the intrinsic efficacy of D_2R ligands, which can explain, for instance, the complete counteraction by $A_{2A}R$ antagonists on MAPK activation and the decrease in neuronal excitability induced by high concentrations of D_2R agonists, which should surmount the reduction in affinity.

More generally, our study calls for an awareness of homodimers as predominant GPCR species, providing a significant role of allosteric interactions between orthosteric ligands within GPCRs and building blocks for heterotetramers (28), which should have important implications in the field of GPCR pharmacology.

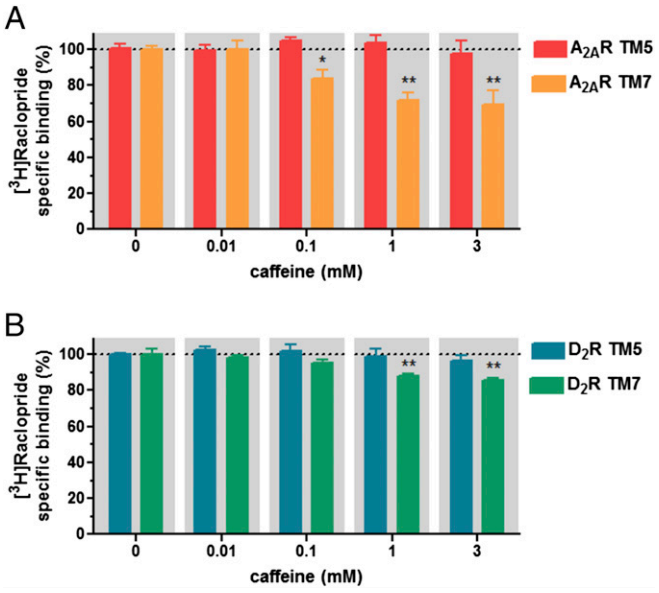

Fig. 8. Effect of HIV TAT-TM peptides on caffeine-induced allosteric modulation of [^{3}H]raclopride binding. Membrane preparations from sheep striatum were pretreated for 2 h with the indicated $A_{2A}R$ (*A*) or D_2R (*B*) HIV TAT peptides (4 μM) and [^{3}H]raclopride (4 nM) binding was performed in the absence or the presence of increasing concentrations of caffeine. Values are means ± SEM from three to five different experiments of the relative [^{3}H]raclopride-specific binding (% of the caffeine untreated membranes). Statistical significance was calculated by one-way ANOVA followed by Dunnett's post hoc test. *$P < 0.05$; **$P < 0.01$, compared with the caffeine-untreated membranes.

Methods

Animals. Male Sprague–Dawley rats (Charles River Laboratories) weighting 300–350 g were used for all experiments. All animals were handled in accordance with the National Institutes of Health's animal care guidelines. The animal research protocol followed for this study (09-BNRB-73) was approved by the National Institute on Drug Abuse Intramural Research Program's Animal Care and Use Committee.

Human Samples. Human brain samples from the nucleus caudate (head area) were obtained by family consent at autopsy in the Basque Institute of Legal Medicine (University of the Basque Country, Bilbao, Spain) from four male subjects without history of neurological or psychiatric disorders and who died suddenly of a car accident. Toxicological screening was negative for all subjects and brain samples were histologically determined as normal. Samples were dissected at the time of autopsy, stored at −70 °C until assay and encoded in order to protect the identity of the subject. The time interval between death and autopsy (postmortem delay at 4 °C) was 26 ± 4 h.

Fusion Proteins and Expression Vectors. Sequences encoding amino acid residues 1–155 and 156–238 of the YFP Venus protein and amino acid residues 1–229 and 230–311 of the RLuc8 protein were subcloned in the pcDNA3.1 vector to obtain YFP Venus (nYFP, cYFP) and RLuc8 (nRLuc, cRLuc) hemitruncated proteins expressed in the pcDNA3.1 vector. Human cDNA for dopamine D_2R (long isoform) and D_1R, adenosine $A_{2A}R$ and A_1R cloned in pcDNA3.1 were amplified without their stop codons using sense and antisense primers harboring either unique EcoRI or BamHI sites. The fragments were then subcloned to be in-frame with the hemitruncated Rluc or YFP into the EcoRI and BamHI restriction sites of the hemitruncated proteins expressing vector, to render the plasmids that express receptors fused to the hemitruncated proteins (D_2R-cYFP, D_2R-cRLuc, $A_{2A}R$-nYFP, $A_{2A}R$-nRluc, D_1R-cYFP, D_1R-cRLuc, A_1R-nYFP, A_1R-nRluc). A peptide derived from the HIV transactivator of transcription, HIV TAT (YGRKKRRQRRRPQ), was fused to a peptide with the amino acid sequence of human A2AR or D_2R TM domains 5 and 7 (TM5 and TM7; Genemed Synthesis 124), to promote integration of the TM domains in the plasma membrane. Because HIV TAT binds to the phosphatidylinositol-(4, 5)-bisphosphate found on the inner surface of the membrane, HIV TAT peptide was fused to the C terminus of TM5 and TM7 to obtain the right orientation of the inserted peptide (2).

Cell Culture and Transient Transfection. CHO and human embryonic kidney (HEK-293) cells were grown in Minimum Essential Medium (MEMα; Gibco) and DMEM (Gibco), respectively, supplemented with 2 mM L-glutamine, 100 μg/mL sodium pyruvate, MEM nonessential amino acid solution (1/100), 100 U/mL penicillin/streptomycin, and 5% (vol/vol) of heat-inactivated FBS (all supplements from Invitrogen). CHO and HEK-293 cells growing in 25-cm^2 flasks or 150-cm^2 dishes were transiently transfected by the polyethilenimine (PEI) method. In brief, cells were incubated for 4 h with the indicated amount of cDNA together with ramified PEI (Sigma-Aldrich; 5 mL of 10 mM PEI for each μg of cDNA) and 150 mM NaCl in a serum-starved medium. After 4 h, the medium was changed to a fresh complete culture medium. Cells were used at 48 h after transfection.

ERK1/2 Phosphorylation Assays. The effect of different ligand combinations on ERK1/2 phosphorylation was studied in HEK-293 cells transfected with $A_{2A}R$ and D_2R. The methodology is described in detail elsewhere (2).

BRET and Bimolecular Bioluminescence and Fluorescence Complementation. HEK-293 cells growing in six-well plates were transiently cotransfected with 1 μg of cDNA encoding for the receptors fused to nRLuc8 and cRLuc8 proteins and with 1 μg of cDNA corresponding to the receptors fused to nVenus and cVenus proteins. To quantify receptor-reconstituted YFP Venus expression, cells (20 μg of total protein per well) were distributed in 96-well microplates (black plates with a transparent bottom), and fluorescence was read in a FLUOstar Optima fluorimeter (BMG Labtech). Receptor fluorescence expression was determined as fluorescence of the sample minus the fluorescence of cells expressing the BRET donor alone. For BRET with bimolecular bioluminescence and fluorescence complementation measurements, cells (10 μg of total protein per well) were distributed in 96-well microplates (Corning 3600 white plates), and 5 μM coelenterazine H (Molecular Probes) was added. At 5 min after the addition of coelenterazine H, the readings were collected using a Mithras LB 940 microplate reader (Berthold Technologies), which allows integration of the signals detected in the short-wavelength filter at 485 nm (440–500 nm) and the long-wavelength filter at 530 nm (510–590 nm). To quantify receptor-reconstituted RLuc8 expression, luminescence readings were also performed at 10 min after the addition of 5 mM coelenterazine H. Both the fluorescence and luminescence of each sample were measured before each experiment to confirm similar donor expression (~150,000 luminescent units). Net BRET was defined as [(long-wavelength emission)/(short-wavelength emission)] − *Cf*, where *Cf* corresponds to [(long-wavelength emission)/(short-wavelength emission)] for the donor construct expressed alone in the same experiment. BRET is expressed as mili BRET units (mBU; net BRET × 1,000).

Radioligand-Binding Experiments. Crude membranes from sheep or human striatum (caudate) or cultured CHO cells were prepared as described elsewhere (23). Protein was quantified by the bicinchoninic acid method (Pierce Chemicals). Binding experiments were performed with membrane suspensions at room temperature in 50 mM Tris·HCl buffer, pH 7.4, containing 10 mM $MgCl_2$ and 0.2 IU/mL adenosine deaminase (EC 3.5.4.4; Roche). For D_2R agonist-binding assays, membrane suspensions (0.2 mg of protein/mL) were incubated with a free concentration (6 nM) of the radiolabeled D_2R agonist [^{3}H]quinpirole (37.2 Ci/mmol; Perkin-Elmer), the indicated concentrations of caffeine (Sigma-Aldrich), the $A_{2A}R$ agonist CGS 21680 (Sigma-Aldrich), and the $A_{2A}R$ antagonist SCH 58261 (Tocris). For D_2R antagonist-binding assays, the medium was supplemented with 120 mM NaCl and 5 mM KCl, and the membrane suspensions (0.2 mg of protein/mL) were incubated with a free concentration (4 nM) of the radiolabeled D_2R antagonist [^{3}H]raclopride (81.9 Ci/mmol; Perkin-Elmer) and the indicated concentrations of caffeine, CGS 21680, or SCH 58261. For experiments with the HIV TAT TM peptides, membranes were preincubated for 2 h with 4 μM of the indicated peptide before the addition of other ligands. For competition experiments, the membrane suspensions were incubated with a constant free concentration of [^{3}H]quinpirole (6 nM) or [^{3}H]raclopride (4 nM) and increasing concentrations of quinpirole (0.01 nM–3 μM) or raclopride (0.01 nM–3 μM), respectively, in the presence or absence of caffeine (3 mM) or CGS 21680 (3 μM). In all cases, free and membrane-bound ligands were separated by rapid filtration, and radioactivity counts were determined as described elsewhere (23).

Two-state dimer model equations were used to determine radioligand-binding parameters, as described in detail elsewhere (29). In dissociation kinetic assays, sheep striatal membranes (0.2 mg of protein/mL) were incubated at 12 °C in Tris·HCl buffer (50 mM, pH 7.4) containing 10 mM $MgCl_2$ and 0.2 IU/mL adenosine deaminase in the absence or presence of CGS 21680 (10 nM), SCH 58261 (10 nM), or caffeine (30 μM). After 30 min, 1.5 nM of the $A_{2A}R$ antagonist [^{3}H]ZM 241385 (50 Ci/mmol; American Radiolabeled Chemicals) was added for an additional 2-h period of radioligand association. Dissociation was initiated by the addition of 10 μM of ZM 241385. At the indicated time intervals, total binding was measured as described above.

Patch-Clamp Recording. Whole-cell patch-clamp recordings were performed on individual neurons from the rat ventral striatum. The method is described in detail elsewhere (9).

Locomotor Activity. Rats received an i.p. injection of 0.1 mg/kg CGS 21680 or vehicle (saline plus 5% DMSO and 5% Tween-80). After 30 min, they received a second i.p. injection of KW 6002 (1, 10, or 30 mg/kg) or vehicle, and locomotor activity was measured by placing the animals individually in motility chambers (50 × 50 cm; Coulbourn Instruments). Locomotion was measured by counting the number of breaks in the infrared beams of the chambers for the first 20 min after the last i.p. injection.

Proximity Ligation Assay. Sheep striatum placed in ice-cold oxygenated (95% O_2/5% CO_2) Krebs-HCO_3^- buffer (124 mM NaCl, 4 mM KCl, 1.25 mM KH_2PO_4, 1.5 mM $MgCl_2$, 1.5 mM $CaCl_2$, 10 mM glucose, and 26 mM $NaHCO_3$; pH 7.4) were dissected and sliced at 4 °C using a brain matrix to obtain 0.5-mm coronal slices. Each slice was transferred to a plate and incubated for 4 h at 30 °C under constant oxygenation in an Eppendorf Thermomixer (5 Primer Inc.) with Krebs-HCO_3^- buffer containing or not containing 4 μM of the indicated HIV TAT TM peptides. Slices were fixed with 4% paraformaldehyde solution for 1 h at room temperature, washed in Tris-buffered saline, and stored at −20 °C in a 30% sucrose solution until sectioning. The 20-μm-thick coronal sections were cut on a freezing cryostat (Leica Jung CM-3000), mounted on glass slides, and permeabilized for 10 min at 4 °C with 0.1% Triton X-100. $A_{2A}R$-D_2R complexes were detected using the Duolink II PLA detection kit (OLink Bioscience) following the manufacturer's instructions using a mixture containing equal amounts of rabbit polyclonal anti-D_2R antibody (1:200, AB5084P; Millipore) and monoclonal mouse anti-$A_{2A}R$ antibody (1:200, 05–717; Millipore). The samples were mounted and observed under a Leica SP2 confocal microscope and processed with ImageJ software. Cells containing one or more spots vs. total cells were determined considering 800–1,000 cells from between five and 12 different fields from three different animals per group using the Fiji package (pacific.mpi-cbg.de) as described previously (30).

ACKNOWLEDGMENTS. We acknowledge the technical assistance of Jasmina Jiménez and Edgar Angelats, and thank Dr. Javier Meana and Dr. Joan Sallés (University of the Basque Country) for providing the human samples. This study was supported by the National Institute on Drug Abuse and grants from the Government of Catalonia (2009-SGR-12), Centro de Investigación Biomédica en Red sobre Enfermedades Neurodegenerativas (CB06/05/0064), and the Spanish Ministerio de Ciencia y Teconolgía (SAF 2011-23813).

1. Ferré S, et al. (2014) G protein-coupled receptor oligomerization revisited: Functional and pharmacological perspectives. *Pharmacol Rev* 66(2):413–434.
2. Guitart X, et al. (2014) Functional selectivity of allosteric interactions within G protein-coupled receptor oligomers: The dopamine D1-D3 receptor heterotetramer. *Mol Pharmacol* 86(4):417–429.
3. Smith NJ, Milligan G (2010) Allostery at G protein-coupled receptor homo- and heteromers: Uncharted pharmacological landscapes. *Pharmacol Rev* 62(4): 701–725.
4. Ferré S, et al. (2009) Building a new conceptual framework for receptor heteromers. *Nat Chem Biol* 5(3):131–134.
5. Ferré S, von Euler G, Johansson B, Fredholm BB, Fuxe K (1991) Stimulation of high-affinity adenosine A2 receptors decreases the affinity of dopamine D2 receptors in rat striatal membranes. *Proc Natl Acad Sci USA* 88(16):7238–7241.
6. Hillion J, et al. (2002) Coaggregation, cointernalization, and codesensitization of adenosine A2A receptors and dopamine D2 receptors. *J Biol Chem* 277(20):18091–18097.
7. Canals M, et al. (2003) Adenosine A2A-dopamine D2 receptor-receptor heteromerization: Qualitative and quantitative assessment by fluorescence and bioluminescence energy transfer. *J Biol Chem* 278(47):46741–46749.
8. Navarro G, et al. (2014) Intracellular calcium levels determine differential modulation of allosteric interactions within G protein-coupled receptor heteromers. *Chem Biol* 21(11):1546–1556.
9. Azdad K, et al. (2009) Dopamine D2 and adenosine A2A receptors regulate NMDA-mediated excitation in accumbens neurons through A2A-D2 receptor heteromerization. *Neuropsychopharmacology* 34(4):972–986.
10. Trifilieff P, et al. (2011) Detection of antigen interactions ex vivo by proximity ligation assay: Endogenous dopamine D2-adenosine A2A receptor complexes in the striatum. *Biotechniques* 51(2):111–118.
11. Ferré S, O'Connor WT, Fuxe K, Ungerstedt U (1993) The striopallidal neuron: A main locus for adenosine–dopamine interactions in the brain. *J Neurosci* 13(12):5402–5406.
12. Ferré S (2008) An update on the mechanisms of the psychostimulant effects of caffeine. *J Neurochem* 105(4):1067–1079.
13. Ferré S, et al. (2004) Adenosine A2A-dopamine D2 receptor-receptor heteromers: Targets for neuro-psychiatric disorders. *Parkinsonism Relat Disord* 10(5):265–271.
14. Armentero MT, et al. (2011) Past, present and future of A(2A) adenosine receptor antagonists in the therapy of Parkinson's disease. *Pharmacol Ther* 132(3):280–299.
15. Ciruela F, et al. (2004) Combining mass spectrometry and pull-down techniques for the study of receptor heteromerization: Direct epitope-epitope electrostatic interactions between adenosine A2A and dopamine D2 receptors. *Anal Chem* 76(18):5354–5363.
16. Woods AS, Ferré S (2005) Amazing stability of the arginine–phosphate electrostatic interaction. *J Proteome Res* 4(4):1397–1402.
17. Navarro G, et al. (2010) Interactions between intracellular domains as key determinants of the quaternary structure and function of receptor heteromers. *J Biol Chem* 285(35):27346–27359.
18. Borroto-Escuela DO, et al. (2010) Characterization of the A2AR–D2R interface: Focus on the role of the C-terminal tail and the transmembrane helices. *Biochem Biophys Res Commun* 402(4):801–807.
19. Bennett KA, et al. (2013) Pharmacology and structure of isolated conformations of the adenosine A_2A receptor define ligand efficacy. *Mol Pharmacol* 83(5):949–958.
20. Doré AS, et al. (2011) Structure of the adenosine A(2A) receptor in complex with ZM241385 and the xanthines XAC and caffeine. *Structure* 19(9):1283–1293.
21. Lebon G, Edwards PC, Leslie AG, Tate CG (2015) Molecular determinants of CGS21680 binding to the human adenosine A2A receptor. *Mol Pharmacol* 87(6):907–915.
22. Ginés S, et al. (2000) Dopamine D1 and adenosine A1 receptors form functionally interacting heteromeric complexes. *Proc Natl Acad Sci USA* 97(15):8606–8611.
23. Orru M, et al. (2011) Striatal pre- and postsynaptic profile of adenosine A(2A) receptor antagonists. *PLoS ONE* 6(1):e16088.
24. Karcz-Kubicha M, et al. (2003) Involvement of adenosine A1 and A2A receptors in the motor effects of caffeine after its acute and chronic administration. *Neuropsychopharmacology* 28(7):1281–1291.
25. Halldner L, et al. (2004) The adenosine A1 receptor contributes to the stimulatory, but not the inhibitory effect of caffeine on locomotion: A study in mice lacking adenosine A1 and/or A2A receptors. *Neuropharmacology* 46(7):1008–1017.
26. Juliano LM, Ferre S, Griffiths RR (2009) The pharmacology of caffeine. *Principles of Addiction Medicine*, eds Ries RK, Fiellin DA, Miller SC, Saitz R (Lippincott Williams & Wilkins, Philadelphia), pp 159–178.
27. Bruce M, Scott N, Lader M, Marks V (1986) The psychopharmacological and electrophysiological effects of single doses of caffeine in healthy human subjects. *Br J Clin Pharmacol* 22(1):81–87.
28. Ferré S (2015) The GPCR heterotetramer: Challenging classical pharmacology. *Trends Pharmacol Sci* 36(3):145–152.
29. Casadó V, et al. (2007) Old and new ways to calculate the affinity of agonists and antagonists interacting with G-protein-coupled monomeric and dimeric receptors: The receptor-dimer cooperativity index. *Pharmacol Ther* 116(3):343–354.
30. Bonaventura J, et al. (2014) L-DOPA treatment in primates disrupts the expression of A(2A) adenosine-CB(1) cannabinoid-D(2) dopamine receptor heteromers in the caudate nucleus. *Neuropharmacology* 79:90–100.